Clinical Immunology 267 (2024) 110349

Contents lists available at ScienceDirect

Clinical Immunology

journal homepage: www.elsevier.com/locate/yclim

Multi-modal immune dynamics of pre-COVID-19 Kawasaki Disease following intravenous immunoglobulin

Nicola Cotugno [a,b,1], Giulio Olivieri [a,c,1], Giuseppe Rubens Pascucci [a,d], Donato Amodio [a,b], Elena Morrocchi [a], Chiara Pighi [a], Emma Concetta Manno [a], Gioacchino Andrea Rotulo [a], Carolina D'Anna [e], Marcello Chinali [e], Isabella Tarissi de Jacobis [f], Danilo Buonsenso [g,h], Alberto Villani [b,f], Paolo Rossi [a,b], Alessandra Marchesi [f], Paolo Palma [a,b,*]

[a] Clinical Immunology and Vaccinology Unit, Bambino Gesù Children's Hospital, IRCCS, Rome, Italy
[b] Chair of Pediatrics, Department of Systems Medicine, University of Rome Tor Vergata, Rome, Italy
[c] PhD Program in Immunology, Molecular Medicine and Applied Biotechnology, University of Rome Tor Vergata, Rome, Italy
[d] Probiomics S.r.l., Via Montpellier 1, 00133 Rome, Italy
[e] Cardiology Unit, Bambino Gesù Children's Hospital, IRCCS, Rome, Italy
[f] Emergency, Acceptance and General Pediatrics Department, Bambino Gesù Children's Hospital, IRCCS, Rome, Italy
[g] Department of Woman and Child Health and Public Health, Fondazione Policlinico Universitario A. Gemelli IRCCS, Rome, Italy
[h] Centro di Salute Globale, Università Cattolica del Sacro Cuore, Rome, Italy

ARTICLE INFO

Keywords:
Kawasaki disease
Proteomics
IVIG
Inflammation
Cytokines
T cells

ABSTRACT

Despite progress, the molecular mechanisms underlying Kawasaki Disease (KD) and intravenous immunoglobulin's (IVIG) ability to mitigate the inflammatory process remain poorly understood. To characterize this condition, plasma proteomic profiles, flow cytometry, and gene expression of T cell subsets were investigated in longitudinal samples from KD patients and compared with two control groups. Systems-level analysis of samples in the acute phase revealed distinctive inflammatory features of KD, involving mainly Th-1 and Th-17 mediators and unveiled a potential disease severity signature. APBB1IP demonstrated an association with coronary artery involvement (CAI) and was significantly higher in CAI+ compared to CAI- patients. Integrative analysis revealed a transient reduction in CD4+ EM T cells and a comprehensive immune activation and exhaustion. Following treatment, Tregs at both frequency and gene expression levels revealed immune dynamics of recovery. Overall, our data provide insights into KD, which may offer valuable information on prognostic indicators and possible targets for novel treatments.

1. Introduction

Kawasaki disease (KD) is the leading cause of acquired heart disease among children in developed countries [1–3]. Approximately 30 % of untreated children may encounter coronary artery involvement (CAI), dropping to 5–7 % in patients who undergo high-dose intravenous immunoglobulin (IVIG) treatment [4,5]. However, the specific mechanisms underlying IVIG's ability to mitigate cardiovascular complications in KD patients remain unclear [6]. In addition, the pathogenesis of KD remains partially elusive, leaving certain aspects of the disease incompletely understood. Previous studies highlighted the pathogenic role of T-cell compartment especially in the initial stages of the disease, where the production of inflammatory cytokines resulting from Th17/Treg cells imbalance plays a pivotal role [7–12]. However, the precise contribution of specific subsets, such as peripheral follicular T helper cells (pTfh), effector memory (EM) and central memory (CM) T cells,

Abbreviation: CAI, Coronary Artery Involvement; CM, Central memory T cells; DEGs, Differential Expressed Genes; DEPs, Differentially Expressed Proteins; EM, Effector memory T cells; FC, Febrile controls; HC, Healthy controls; IVIG, intravenous immunoglobulin; KD, Kawasaki Disease; LAD, Left Anterior Descending coronary artery; LM, Left Main Coronary Artery; PCA, Principal component analysis; pTfh, peripheral follicular T helper cells; RCA, Right main Coronary Artery; TEMRA, Terminally differentiated effector memory T cells; Treg, regulatory T cells.

* Corresponding author at: Bambino Gesù Children's Hospital, IRCCS, Piazza Sant'Onofrio 4, 00165 Rome, Italy.
E-mail address: paolo.palma@opbg.net (P. Palma).

[1] These Authors contributed equally to the present manuscript

https://doi.org/10.1016/j.clim.2024.110349
Received 11 June 2024; Received in revised form 21 August 2024; Accepted 22 August 2024
Available online 24 August 2024

remains controversial [8–10]. Furthermore, limited knowledge currently exists regarding the IVIG effects on specific T-cell populations at both frequency and gene-expression levels. Previous studies have attempted at finding possible transcriptional characteristics identifying genes of interest for KD diagnosis [13]. Although such data have provided a crucial advance in understanding this condition, a multi modal longitudinal analysis following immune modulation treatment is missing. To address these gaps and enhance insights into KD's pathogenesis, we performed a comprehensive analysis of the immune profile of KD children before and after IVIG therapy and compared with those of controls.

2. Materials and methods

2.1. Sex as a biological variable

Our study examined male and female participants, and similar findings are reported for both sexes.

2.2. Study participants, samples collection and study approval

We recruited KD Caucasian children during the acute febrile stage as well as age-sex matched healthy controls (HC), and febrile controls (FC) at Bambino Gesù Children's Hospital (BGCH) in Rome between March 2017 and January 2020. For KD children fever onset was considered as the first day of the acute phase. Blood samples from KD patients and FC (infectious diseases of FC were detailed in Table S1) were collected at the time of admission before any antibiotic or/and anti-inflammatory therapies administration. KD blood samples were collected at diagnosis (T0), 48 h (T1) and 4 weeks after IVIG therapy (T2) (Fig. 1A).

According to the Italian Society of Pediatric [14], and American Heart Association (AHA) guidelines [3] IVIG infusion has been performed in 10–12 h if patient's cardiac function is normal or in 16–24 h for patients displaying cardiac failure. IVIG resistance was defined as persistent or recrudescent fever at least 36 h and < 7 days after completion of first IVIG infusion.

Two-dimensional echocardiographic examination was performed for all KD patients at onset. The internal diameter of the left main (LM) coronary artery, the left anterior descending (LAD), and the right main coronary artery (RCA) were measured and expressed as *Z*-score (SD units from the mean normalized for body surface area). CAI was defined according to the AHA guidelines [3], which classify Z-Score value as follows: a) no involvement: <2; b) dilation: from 2 to <2.5; c) small aneurysm: ≥2.5 to <5; d) medium aneurysm: ≥5 to <10, and absolute dimension <8 mm; e) large or giant aneurysm: ≥10, or absolute dimension ≥8 mm. Patients with Z-scores ≥2 for any coronary artery were considered to be CAI+, patients without as CAI-.

The BGCH Ethics Committees approved the study (protocol 1376_OPBG_2017) and informed consent was obtained from all parents prior to inclusion. All patients were included in accordance with study protocol, the International Conference on Harmonization Good clinical Practice guidelines, and the provisions of the Declaration of Helsinki.

2.3. Proteomic assay

Plasma samples were analyzed using the Olink Inflammation and

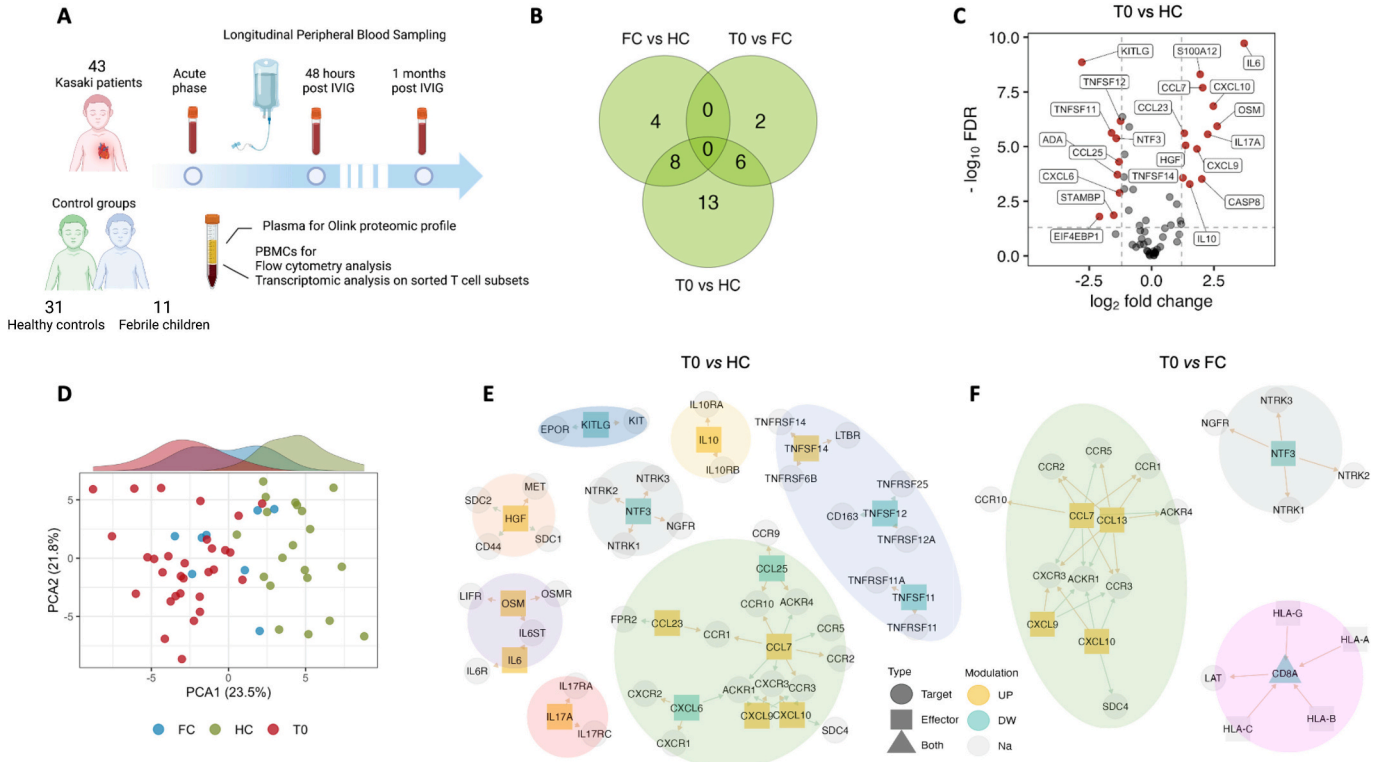

Fig. 1. Proteomic profiling and Exploring Network Analysis.
(A) Schematic of the longitudinal study design, involving KD patients and two cohorts of controls.
(B) Venn diagram highlights the common number of proteins found differentially expressed across KD patients and the control groups.
(C) Volcano plot showing DEPs between Kawasaki Disease acute patients and Healthy controls.
(D) Principal component analysis of inflammatory proteins allows to distinguish acute KD from the control groups.
(E) Protein-protein interaction network analysis showing upregulated (yellow) or repressed (light blue) proteins and their function [target (cycle), effector (square) or both (triangle)] in KD children versus healthy controls and F) febrile controls. The relationships between pathways and DEP nodes, as well as their regulatory mode (positive or negative), were sourced from the Omnipath database. (For interpretation of the references to colour in this figure legend, the reader is referred to the web version of this article.)

Cell Regulation 96-plex panels based on the highly sensitive and specific proximity extension assay technology [15]. Briefly, each target protein was recognized by double antibodies and coupled with its specific complementary DNA barcode, which was subsequently quantified using a high throughput microfluidic real-time PCR instrument, Biomark HD (Fluidigm, South San Francisco, CA). To reduce variations between different runs of the experiment and within each run, the data underwent a normalization process. This involved the utilization of two control measures: an internal control (also known as an extension control) and an inter-plate control. The pre-processed data were reported in arbitrary units as Normalized Protein Expression (NPX) that enables individual protein analysis across a sample set analyzed in log2 scale, wherein a higher NPX correlates with higher protein expression. The data were pre-processed using the NPX Manager Software and Olink Analyze R package (version 1.3.0). Proteins exhibiting values below the limit of detection (LOD) in over 80 % of cases were excluded from the dataset. To streamline research and enrichment analyses in public databases, the Olink protein names were substituted with their corresponding official gene symbols.

2.4. Flow cytometry analysis of T subsets in KD patients and control groups

Isolated PBMC were first stained with LIVE/DEAD™ Fixable Near-IR Dead Cell Stain Kit (for 633 or 635 nm excitation, ThermoFisher, Waltham, Massachusetts, US) for 15 min at room temperature (RT). Then, the cells were washed in wash buffer (phosphate-buffer saline with 1 % bovine serum albumin) and stained for 30 min at 4 °C with anti-hCD3 PE-CF594, anti-hCD4 BV510, anti-hCD25 PE, anti-hCD45RO-PerCP-Cy 5.5, anti-hCD27 V450, anti-hCD57 APC, anti-hCXCR5 BV605 (all from BD Biosciences, Milan, Italy), anti-hCD127 PE-Cy7, anti-hPD1 BV786 (all from Biolegend, San Diego, CA). After incubation, superficially stained cells were washed and fixed with 1 % PFA (phosphate-buffer saline with 1 % paraformaldehyde) at RT for 10 min. Washed cells were permeabilized with 1 % Permeabilizing Solution 2 (BD Biosciences, Milan, Italy) and incubate for 10 min at RT. Intracellular detection of FoxP3 with anti-hFoxP3 AF488 (Biolegend, San Diego, CA) was performed incubating for 30 min at 4 °C. The gating strategy to identify T cell subsets (CD3 + CD4+), comprising Regulatory T cells (Treg, CD4 + CD25 + CD127low), Central memory T cells (CM, CD4+ CD45RO+ CD27+), Effector memory T cells (EM, CD4+ CD45RO+ CD27-), memory T cells re-expressing CD45RA (TEMRA, CD4+ CD27-CD45RO) and pTfh (CD4+ CD45RO+ CD27+, CXCR5+). The gating strategy is shown in supplementary Fig.S1.

Data acquired by CytoFLEX cytometer (Beckman Coulter, Milan, Italy) were analyzed by FlowJo software v.10 (Treestar Software, Ashland, Oregon, USA). Statistical comparisons were performed with paired or unpaired nonparametric Mann-Whitney *U* test or *t*-test.

2.5. Cell sorting and RNA extraction

Cryopreserved PBMC from T0, T1 and T2 were thawed, stained for the following previously titrated surface antibodies: hCD3 PE-CF594, anti-hCD4 BV510, anti-hCD25 PE, anti-hCD45RO-PerCP-Cy 5.5, anti-hCD27 V450 (all from BD Biosciences, Milan, Italy), anti-hCD127 PE-Cy7 (Biolegend, San Diego, CA) and sorted by FACSAriaII (BD Biosciences). LIVE/DEAD™ Fixable Near-IR Dead Cell Stain Kit (for 633 or 635 nm excitation, ThermoFisher, Waltham, Massachusetts, US) was used to determine viability of the cells. Five hundred live cells per T cell subset were sorted in tubes previously loaded with 9 μL of CellsDirect one-step polymerase chain reaction (PCR) buffer and pooled TaqMan gene expression assays (2× CellsDirect Reaction mix 5 μL, Superscript III + Taq polymerase 0.5 μL, 0.2× TaqMan primer pool 2.5 μL, Resuspension Buffer 1 μL). After sorting Tregs, CM and EM CD4+ T cells, samples were transferred to PCR tubes and reverse transcription and target-specific preamplification was performed on a C1000 Thermal Cycler (BioRad) with the following scheme (50 °C for 20 min, 95 °C for 2 min, 95 °C for 15 s, 60 °C for 4 min, last two steps repeated for 18 cycles). Resulting cDNA was stored at −20 °C until further analysis.

2.6. Multiplexed RT-PCR

Previously amplified samples were loaded on a Fluidigm 96.96 standard chip following manufacturer's instructions, as previously described [16]. All TaqMan primers/ probes used for the gene mix were selected according to literature, online gene banks and biological queries. The sorting experiments and BioMark experiments were randomized to include a mix of HC, KD, and FC patient samples to avoid bias. Genes and samples exceeding 40 % and 20 % of flagged values, respectively, were removed from the dataset. Expression threshold values were normalized doubling the weight of the housekeeping gene CD74 included in our panel [17]. Differential analysis was performed using the limma package and only genes with an adjusted p-value <0.05 and a log2 fold change >1.2, in absolute value, were considered as Differential Expressed Genes (DEGs).

2.7. Statistical analysis

Normality for continuous variables was assessed using the Shapiro test. Proteomics and clinical variable comparison employed one-way ANOVA followed by Tukey-Kramer's post hoc test for normally distributed and homogeneous distributions. For comparisons between two groups, we used the *t*-test, Welch t-test, and Mann-Whitney test. Results were considered statistically significant for variables with an adjusted p-value (adj) < 0.05. A ranking plot [−log10(Adjusted p-value) * log2(Fold Change)], was used to emphasize the magnitude of the difference. The multiple comparisons were adjusted using False Discovery Rate (FDR).

Differential expressed proteins (DEPs) functions were analyzed with KEGG pathway enrichment (enrichr v3.2) [16] and explored protein-protein interactions (PPI) using OmnipathR v3.2 [18].

Principal Component Analysis (PCA) on proteomics data was utilized to assess patient distribution. Moreover, to integrate laboratory parameters, flow cytometry, and proteomics data we applied Multi-Omics Factor Analysis (MOFA) using the MOFA2 R package [19]. MOFA is an integration method catching the common variability among the datasets provided as input. MOFA calculates factors made up of a linear combination of the multi variables and selects the most relevant contributors after discarding the not relevant ones by regularization. Spearman's correlation was used to examine the associations between variables.

All statistical analyses were performed using R (version 4.1.1).

2.8. Machine learning

To investigate KD key proteins and to build a model able to correctly classify KD patients based on these features, we applied a Machine Learning (ML) approach.

To reduce the overfitting risk caused by the small sample size, we selected the 13 DEPs exclusively different in the KD group against the subjects of all other groups. After a preprocessing step, this dataset was split into training (60 %, 35 subjects) and testing (40 %, 23 subjects) datasets. The choice of a 60 % training and 40 % testing split for our ML dataset was made to ensure a balance between sufficient training data and robust evaluation [20]. Four ML algorithms were used, including Logistic Regression, Random Forest, eXtreme Gradient Boosting (XGBoost) and k-nearest neighbor (kNN). Accuracy, sensitivity, and specificity computed on the testing dataset were used to evaluate the models (Table S2). XGBoost (XGB) classification algorithm, which is a scalable end-to-end tree boosting system that can and capture non-linear relationships between the features and the target variable, was chosen for the construction of the final model. Notably, this tool has been already used to differentiate patients with KD from controls using

routine laboratory parameters. [21]

3. Results

Forty-three acute KD children, thirty-one HC and eleven FC were recruited. Demographic data, routine laboratory parameters, echocardiogram data as well as differences in these parameters among groups are summarized in Table 1. Clinical features observed in KD patients were reported in Table S3. At disease onset, 11 KD patients (25.6 %) exhibited CAI. Forty-one patients (95.3 %) responded favorably to IVIG infusion (2 g/kg of body weight) while two patients received a second infusion due to persistent fever post treatment.

3.1. Unravelling the proteomic profile of Kawasaki disease

To explore the proteomic profile of KD, we investigated 180 plasma proteins at baseline, at T1 and at T2 as in the control groups. The analysis revealed a distinctive signature consisting of 27 DEPs between acute KD and HC (Fig. 1B). Of these, the majority (21 DEPs; Fig. 1C) were linked to inflammatory processes aligning with previous reports [22–25], while 6 additionally DEPs (APBB1IP, LRRN1, CBL, KAZALD1, IRAG2, DKKL; Fig. S2A) predominantly contributed to immune regulation response. The analysis revealed a KD proteomic signature when compared to FC made of 8 DEPs, 6 of which overlapped with the KD vs HC comparison (Fig.S2B). Indeed, KD patients displayed higher levels of CXCL9, CXCL10, CCL7, CCL13 and reduced levels of NTF3, ADA, EIF4EBP1 and CD8A when compared to FC. Principal component analysis (PCA) of the protein dataset was able to distinguish KD from FC suggesting a distinct inflammatory proteomic profile between the two conditions (Fig. 1D). To further investigate the plasma proteomic signatures identified in KD children from a functional and qualitative perspective we employed Protein-protein interaction (PPI) network analysis and Gene Ontology (GO) and KEGG enrichment analysis. The PPI network highlighted 8 main clusters when comparing the proteomic profile of KD with HC (Fig. 1E) and 3 clusters when comparing KD to FC (Fig. 1F). In both comparisons, predominance of cytokine-chemokine mediated signaling pathways, showing the roles of CXCL9 and CXCL10 and highlighting the central role of chemokine CCL7.

In comparison to HC, KD children also exhibit several TNFSF proteins which regulate various aspects of the immune system, cell survival and inflammatory cytokine pathways such as IL-6 and IL-17 [26]. KEGG enrichment analysis, showed that DEPs in KD present a significant enrichment in cytokine-cytokine receptor, chemokine signaling pathways, IL-17 signaling pathway and PI3k-Akt signaling pathway (Fig. S2C). Moreover, KD patients also showed DEPs mainly enriched in cell chemotaxis, leukocyte migration, cytokine-mediated signaling pathway and response to chemokines when compared to FC (Fig. S2D).

3.2. Prognostic indicators

To enhance our understanding of Kawasaki disease's pathogenesis and unveil potential prognostic indicators, we conducted correlation analyses integrating laboratory parameters, echocardiogram values and proteomics in KD. Our analysis identified an inverse correlation between age and an array of proteins including CASP8, OSM, TGFA, TNFSF14, EIFEBP1, APBB1IP, and STAMBP (Fig. 2A). Furthermore, we found a negative correlation linking CCL13 with ferritin, AST levels, and intriguingly, with RCA values. Regarding echocardiographic parameters, we identified a positive correlation between APBB1IP levels and the maximum *Z*-score (any dilated coronary artery; $p = 0.001$, $r = 0.66$;), as well as with the LAD values expressed in mm ($p = 0.04$, $r = 0.47$). A full list of echocardiogram values of patients presenting with CAI has now been shown in Table S4. The association between APBB1IP and CAI was also confirmed by a preliminary analysis showing a significantly higher protein level in CAI+ as compared to CAI- patients ($p = 0.00183$, Fig. S2E).

3.3. Longitudinal analysis reveals the proteomic dynamics after IVIG in KD

The effect of IVIG on KD proteomic profile was investigated by longitudinal analysis. PCA segregated well KD samples collected in distinct time-points suggesting that proteomic dynamics were able to characterize the effect of IVIG intervention (Fig. 2B). Top contributing features for PCA are reported in Fig. 2C. Following IVIG infusion, a significant decline was observed in various proteins, each exhibiting a distinct kinetic pattern. Notably, TNFRSF10A and CCL23 exhibited an initial and significant reduction at T1, which was followed by a sustained decrease at T2, reaching levels comparable to those observed in HC (Fig. 2D). Conversely, several cytokines exhibited a gradual decline, with statistically significant differences emerging only at T2 when compared to both T0 and T1. This trend was exemplified by IL-6, IL-17 A, IL-17C, CXCL11, CXCL10, CXCL9, CCL23, TNF and others (Fig. 2D, Fig.S3A). IVIG was also able to reduce VEGFA levels, a protein associated with angiogenesis and vasculogenesis which resulted previously correlated with CAI in KD patients [27]. Therapy also resulted in a decrease in the two proteins positively associated with echocardiogram values (CCL13 and APBB1IP) (Fig.S3B).

On the other hand, IVIG increased the levels of TNFSF11, NTF3, CD6, LRRN1, TAFA5, DCBLD2, ZBTB16, and KAZALD1 (Fig. S3C). Whereas the proteomic profile mainly overlapped between convalescent KD and HC, a downregulation of EIF4EBP1, AXIN1, IFNG, SIRT2, STAMBP, ADA, CD8A, IL17C, and DKKL1, along with an increase in CASP8 levels (Fig.S3D) was found between T2 and HC suggesting that an aspecific inflammatory perturbation may persist after clinical recovery.

3.4. Flow cytometry of T-cell compartments in acute phase and post IVIG treatment

To enhance our understanding of KD pathogenesis, in line with the proteomic results which highlighted the role of proteins involved in T cell regulation we investigated the T cell compartment by flow cytometry analysis in longitudinal samples.

The analysis of memory CD4+ T-cells subsets showed significantly lower frequency of EM and TEMRA subsets compared to FC ($p = 0.006$; $p = 0.01$ respectively) (Fig. 3A). Compared to HC, KD and FC showed lower percentage of both naïve T-cells and T CD4+ CM cells (KD vs HC: $p = 0.025$, $p < 0.001$ respectively; HC vs FC: $p = 0.025$; $p = 0.03$). In addition, a lower frequency of pTfh cells was observed in both KD and FC groups respect the HC group ($p = 0.015$; $p = 0.012$ respectively). KD children exhibited a higher percentage of PD1 + Treg+ cells compared to FC subjects ($p < 0.001$; Fig. 3A). We further explored the T-cell subsets dynamics in KD cells at T1 and T2. The percentage of Tregs cells significantly increased following IVIG therapy at both time points compared to baseline ($p = 0.013$; $p = 0.006$, respectively; Fig. 3B). Conversely, the CM cells populations exhibited a gradual rise, culminating at T2 ($p = 0.004$) with value like HC. The levels of PD1+ Treg cells showed a decreasing trend although a significant difference was not achieved. Interestingly, performing a correlation analysis we found an inverse correlation between this peculiar cell subset and the levels of OSM, TGFA, and APBB1IP (Fig. 3C).

3.5. Distinct T cells gene expression pattern between KD children and control groups

To further explore the T-cells compartment we investigated gene expression in sorted EM, CM and Treg cells. Differential analysis between KD and FC, revealed 17 DEGs, 11/17 within the EM subset and 6/17 within the CM T-cells subset (Fig. 3D, Fig. 3E), suggesting that qualitative perturbation, identified by transcriptional analysis, coupled with quantitative T-cell subsets analysis may define distinctive signatures of KD.

We further investigated whether there were any individual-level

Table 1
Clinical characteristics of enrolled patients and controls. Demographic, laboratory parameters, and echocardiogram data of our cohort at baseline and throughout the follow-up period. The Mann-Whitney *U* test was used to compare median values across groups of children, and the same test was also used to compare distributions of clinical data.

	T0 Acute onset ($n = 43$)	T1 48 h post IVIG ($n = 30$)	T2 1 month post IVIG ($n = 17$)	FC ($n = 11$)	HC ($n = 31$)	*P* value
Gender (F:M)	19:24	11:19	8:9	5:6	16:15	
Age, median (range), years	1.93 (0.37–7.15)	2.12 (0.38–7.16)	1.74 (0.78–7.24)	2.05 (0.19–5.38)	2.82 (0.55–7.8)	
Red Blood Cells, median (range), 10^6/microL)	4.05 (3.15–5.67)	4.01 (3.51–5.36)	4.41 (4.07–5.71)	4.62 (3.09–5.27)	4.81 (4.36–5.58)	$p < 0.001$ (T0 vs HC), $p < 0.001$ (T1 vs HC), $p = 0.0303$ (T2 vs T0), $p = 0.046$ (T2 vs HC)
Hemoglobin, median (range), g/dL	10.75 (8–12.7)	10.3 (8.5–12.8)	11.5 (10.3–13.6)	11.9 (9–13.1)	12.3 (10.9–14.7)	$p < 0.001$ (T0 vs HC), $p < 0.001$ (T1 vs HC), $p = 0.0228$ (T2 vs T0), $p = 0.0244$ (T2 vs T1)
Hematocrit, median (range), %	32.6 (26.9–39.6)	32.1 (27.7–38.9)	36.45 (29.1–40.7)	35.1 (27.1–38.4)	37.6 (34.3–42.2)	$p < 0.001$ (T0 vs HC), $p < 0.001$ (T1 vs HC), $p < 0.001$ (T2 vs T0), $p = 0.0028$ (T2 vs T1), $p = 0.0114$ (FC vs HC)
White Blood Cells, median (range), 10^3/microL	13.38 (4.51–23.82)	8.8 (4.94–20.27)	7.92 (5.15–30.04)	14.73 (4.97–21.83)	7.93 (0.36–11.84)	$p < 0.001$ (T0 vs HC), $p = 0.0013$ (FC vs HC), $p = 0.0082$ (T2 vs T0), $p = 0.0176$ (T1 vs T0), $p = 0.0256$ (T2 vs FC)
Neutrophils, median (range), 10^3/microL	8.91 (1.34–17.13)	4.66 (1.31–14.58)	3.29 (1.77–23.61)	6.66 (1.91–15.76)	2.67 (0.9–6.11)	$p < 0.001$ (T0 vs HC), $p < 0.001$ (T2 vs T0), $p < 0.001$ (FC vs HC), $p = 0.0031$ (T1 vs T0), $p = 0.0049$ (T2 vs FC), $p = 0.0081$ (T1 vs HC)
Lymphocytes, median (range), 10^3/microL	2.92 (0.29–8.86)	3.2 (0.99–11.35)	4 (2.46–8.28)	3.38 (2.22–6.96)	4.08 (1.5–5.89)	
Monocytes, median (range), 10^3/microL	0.48 (0.1–1.55)	0.53 (0.23–1.34)	0.46 (0.3–1.26)	1.22 (0.21–2.19)	0.43 (0.22–1.28)	$p = 0.0114$ (FC vs HC)
Eosinophils, median (range), 10^3/microL	0.3 (0.01–1.33)	0.31 (0.01–0.89)	0.26 (0.09–0.9)	0.15 (0.01–0.58)	0.16 (0.03–0.71)	
Basophils, median (range), 10^3/microL	0.04 (0.01–0.13)	0.05 (0.01–0.24)	0.06 (0.02–0.18)	0.04 (0.03–0.29)	0.04 (0.01–0.09)	
Platelets, median (range),10^3/microL	409.5 (82–811)	601 (269–1069)	334.5 (168–985)	466 (210–550)	355 (220–563)	$p < 0.001$ (T1 vs HC), $p = 0.002$ T2 vs T1), $p = 0.002$ (T1 vs T0), $p = 0.0083$ (T1 vs FC)
Neutrophils, median (range), %	67.75 (11.1–87.4)	53.6 (16.8–82.2)	40.45 (23.5–78.6)	58.7 (35.2–74.9)	37.7 (16.3–63.6)	$p < 0.001$ (T0 vs HC), $p < 0.001$ (T2 vs T0), $p = 0.003$ (FC vs HC), $p = 0.0088$ (T1 vs T0), $p = 0.0148$ (T1 vs HC), $p = 0.0197$ (T2 vs FC)
Lymphocytes, median (range), %	22.65 (4.6–73.3)	35.4 (13.8–71.6)	44.8 (15.3–64)	29.8 (14.8–44.6)	52.2 (17.2–69.8)	$p < 0.001$ (T0 vs HC), $p < 0.001$ (T2 vs T0), $p < 0.001$ (FC vs HC), $p = 0.005$ (T1 vs HC), $p = 0.0119$ (T1 vs T0), $p = 0.0168$ (T2 vs FC)
Monocytes, median (range), %	3.95 (1.8–10.9)	5.6 (2.1–12)	5.5 (4.2–10.2)	8.3 (2.6–13.5)	5.4 (3.4–12.1)	$p = 0.0158$ (T0 vs FC)
Eosinophils, median (range), %	2.65 (0.2–9.1)	2.8 (0.1–11)	3.3 (0.3–9.4)	1.1 (0.1–3.6)	2.25 (0.4–7.8)	
Basophils, median (range), %	0.3 (0.1–1.1)	0.5 (0.1–1.9)	0.6 (0.3–1.1)	0.5 (0.2–1.5)	0.6 (0.3–1)	$p < 0.001$ (T0 vs HC), $p = 0.002$ (T2 vs T0), $p = 0.002$ (T1 vs T0)
C-Reactive Protein, median (range), mg/dL	10.48 (0.5–29.33)	2.97 (0.64–15.59)	0 (0–1.91)	10.41 (0.78–19.32)	0.01 (0–1.9)	$p < 0.001$ (T0 vs HC), $p < 0.001$ (T2 vs T0), $p < 0.001$ (FC vs HC), $p < 0.001$ (T1 vs HC), $p = 0.0188$ (T1 vs T0), $p < 0.001$ (T2 vs FC), $p < 0.001$ (T2 vs T1),
Ferritin, median (range), ng/mL	205 (95–1270)	188 (73–315)	41 (16–419)	196 (49–494)	20 (5–81)	$p < 0.001$ (T0 vs HC), $p < 0.001$ (T1 vs HC), $p = 0.0015$ (T2 vs T0), $p = 0.0046$ (FC vs HC), $p = 0.0099$ (T2 vs T1)
Sodium, median (range), mEq/L	136 (130–143)	136 (132–138)	137 (134–139)	137.5 (135–139)	139 (134–142)	$p < 0.001$ (T0 vs HC), $p < 0.001$ (T1 vs HC)
Potassium, median (range), mEq/L	4.56 (0.25–5.96)	5 (3.34–6.04)	5.03 (4.35–5.37)	4.72 (3.68–5.92)	4.64 (0.2–5.83)	
Calcium, median (range), mg/dL	9.1 (7.3–9.8)	9.1 (7.9–10)	10.2 (9.6–10.9)	9.1 (8.9–9.5)	10.1 (9.3–11.2)	$p < 0.001$ (T2 vs T0), $p < 0.001$ (T0 vs HC), $p < 0.001$ (T2 vs T1), $p = 0.002$ (T1 vs HC), $p = 0.0035$ (T2 vs FC), $p = 0.0099$ (FC vs HC)
Glucose, median (range), mg/dL	94.5 (75–131)	76 (70–94)	76 (63–94)	88.5 (72–105)	78 (55–112)	$p < 0.001$ (T0 vs HC), $p < 0.001$ (T2 vs T0), $p = 0.0339$ (T1 vs T0)
Aspartate Aminotransferase, median (range), U/L	29 (14–87)	32 (18–168)	36.5 (26–43)	34.5 (19–82)	35 (23–75)	
Alanine Aminotransferase, median (range), U/L	29 (8–275)	18 (8–90)	17 (7–48)	18.5 (6–47)	17 (9–35)	$p = 0.0164$ (T0 vs HC)
Gamma-glutamyl Transferase, median (range), U/L	18 (3–139)	19 (3–58)	11 (5–91)	10 (7–45)	10 (2–38)	
Bilirubin, median (range), mg/dL	0.23 (0.11–0.63)	0.18 (0.15–0.37)	0.28 (0.16–0.51)	0.15 (0.15–0.27)	0.29 (0.15–1.16)	
Albumin, median (range), g/dL	3.7 (2.5–4.8)	3.35 (2.4–4.1)	4.5 (4–5)	3.9 (3.7–4.2)	4.6 (4.1–5.1)	$p < 0.001$ (T1 vs HC), $p < 0.001$ (T0 vs HC), $p < 0.001$ (T2 vs T1), $p < 0.001$ (T2 vs T0), $p = 0.011$ (FC vs HC)
LM, median (range), mm	27 (2–39)	25.5 (17–34)	23 (13−31)	NA	NA	
Z-SCORE, median (range)	1.25 (−2.29–5.4)	0.91 (−2.2–5.4)	0.42 (−1.64–1.5)	NA	NA	
LAD, median (range), mm	19 (1–29)	19.5 (10–27)	17 (12–26)	NA	NA	
RCA, median (range), mm	22 (1−31)	20.5 (10–26)	19 (13–25)	NA	NA	

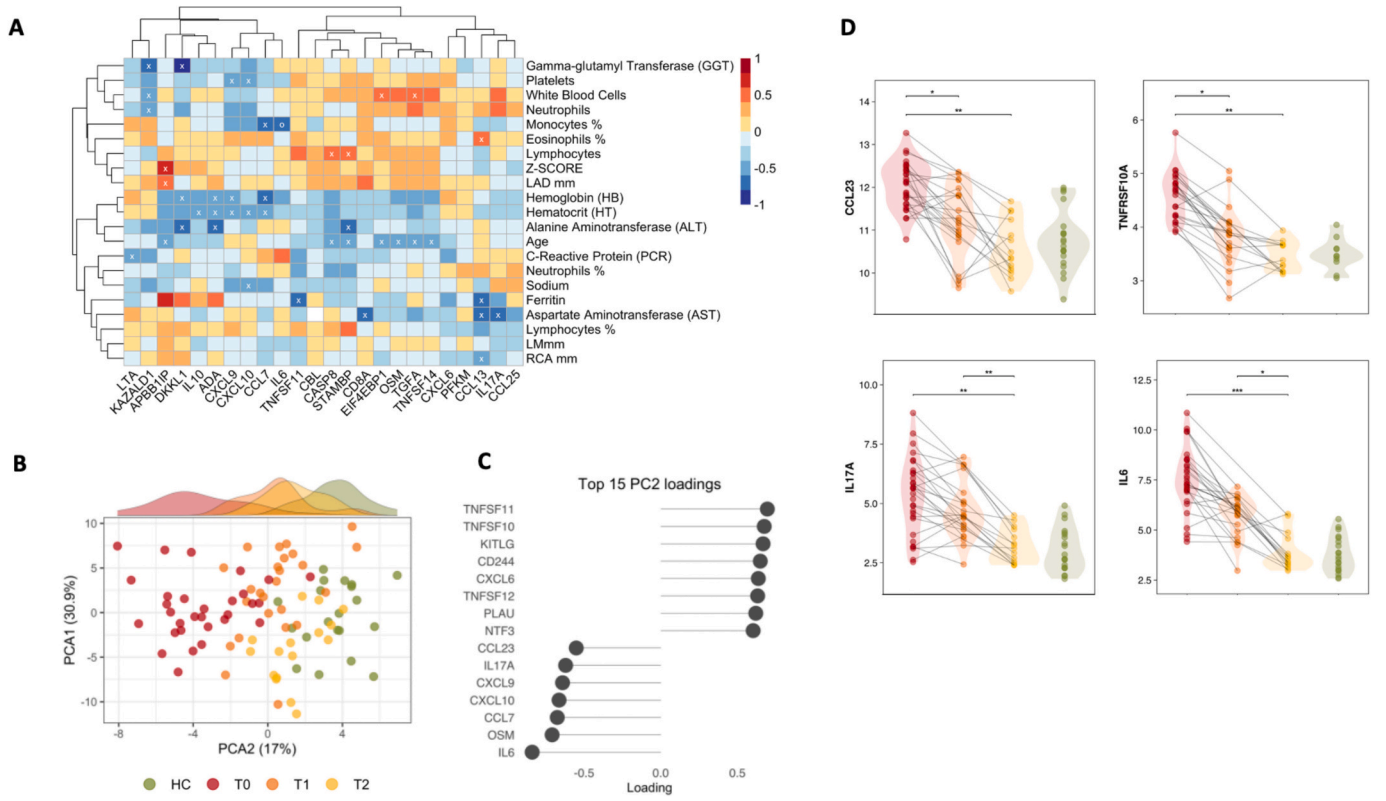

Fig. 2. Proteomic Analysis in KD patients: Clinical Correlation and Longitudinal Investigation.
(A) Heat map illustrating positive correlations (in red) and negative correlations (in blue) between proteins, laboratory parameters, and echocardiogram values in children with Kawasaki Disease. 'X' represents *p*-values <0.05, while 'O' signifies p-adjusted values <0.05.
(B) Principal component analysis (PCA) of inflammatory proteins allows to distinguish acute KD patients from those who received IVIG treatment.
(C) Top contributing features for PCA2.
(D) Proteomics longitudinal analyses of KD at the three time points analyzed compared to HC. Violin plots represent the group's distribution. Each line between KD timepoints represents the protein level trajectory for an individual patient. We present the two proteins (CCL23 and TNFRSF10A) that showed a significant reduction at both T1 and T2 respect baseline and changes in IL6, IL17A value which showed a decreasing kinetic pattern at both T0 and T1 when compared to T2. The pre-processed data were reported in arbitrary units as Normalized Protein Expression (NPX) that enables individual protein analysis across a sample set analyzed in log2 scale, wherein a higher NPX correlates with higher protein expression. * p-adjusted value <0.05, ** p-adjusted value <0.01; *** p-adjusted value <0.001. (For interpretation of the references to colour in this figure legend, the reader is referred to the web version of this article.)

gene expression changes in CM, EM, and Treg following IVIG infusion. In this light, we performed paired analysis using data from each participant. In EM compartment this analysis revealed that 2 genes (*IFNAR2, TGFB1*), both involved in the regulation of T cells functions, were upregulated after one month of IVIG infusion (Fig. 3F). In the Treg compartment, we found a strong upregulation of *NFATC1* (*Nuclear Factor of Activated T Cells 1*) (Fig. 3F) which controls many activation, proliferation, and differentiation pathways of T cells [28,29]. In conclusion, our findings affirm the impact of IVIG on Treg cells and highlight its impact on EM cells at transcriptional level.

3.6. Multi omics integration analysis to comprehensively characterize Kawasaki disease

MOFA was used to integrate laboratory parameters, frequencies of T cell subsets, and plasma protein concentrations derived from both KD patients and control groups.

We identified 7 latent factors that elucidate the combined variances present within the routine laboratory analysis, cellular compositions, and protein datasets (Fig.S4A, Fig.S4B). The first factor, mainly informed by routine laboratory analysis and proteomics, distinctly segregates KD during both acute and convalescent phases and from the control groups. The top three laboratory features enabling the differentiation between KD and controls were: CRP levels, ferritin levels, and the absolute neutrophil count (Fig.S4C). Conversely, factors showing a negative association included both the absolute number and percentage of lymphocytes. Among proteins the top five markers were inflammatory cytokines: IL-6, OSM, CXCL10, IL-17 A and CCL7 (Fig.S4D). In contrast, the key proteins negatively associated with KD were KITLG and TNFSF11 (Fig.S4E).

3.7. Machine learning model highlighted potential key protein

To obtain more precise information about proteins that might be useful in clinical practice we used a mathematical model approach. Leveraging machine learning techniques, we successfully identified the key contributing features that account for the distinctions between KD and the other groups (Fig. 4A). This mathematical model showed an accuracy of 0.87, a specificity of 0.91, and a sensitivity of 0.83 (Fig. 4B). In Fig. 4C were reported proteins ordered by importance within the model. We found that CXCL10, IL-17 A and IL-10 contributed most to the cytokine storm of KD. Both CXCL10 and IL-17 A are key mediators secreted in response to pro-inflammatory signals, serving critical roles in attracting activated Th1 and Th17 cells to the sites of inflammation [30–33]. In contrast, the top negative contributor was TNFSF12 *(TNF Superfamily Member 12)* that has multiple biological activities, including stimulation of microvascular growth and angiogenesis, endothelial cells proliferation, induction of inflammatory cytokines and stimulation of apoptosis [34]. While this approach was constrained by the limited sample size and the accompanying risk of overfitting, it suggests the

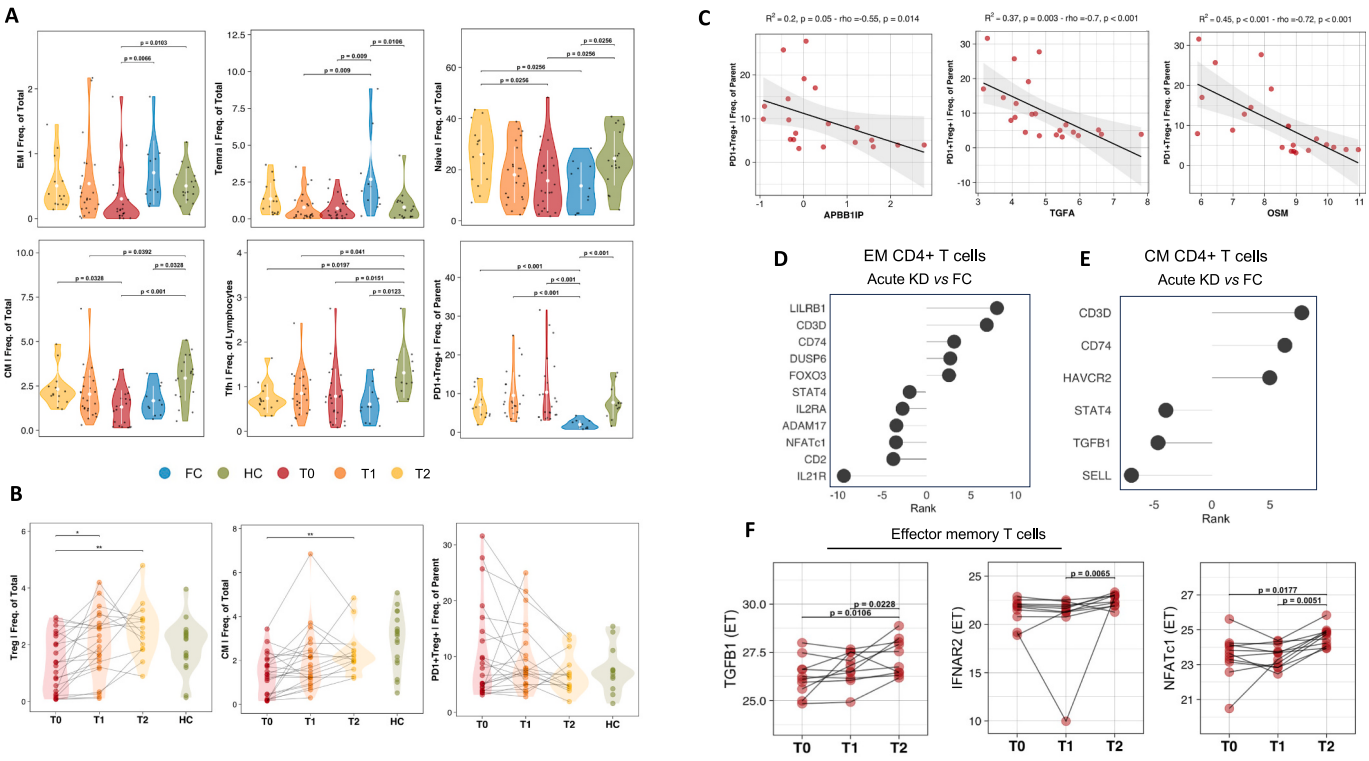

Fig. 3. Evaluation of T Cell Subsets, Post-Therapy Alterations, and Transcriptomic Profiles in KD Children.
(A) Violin plots illustrating differences in cellular T subsets in children with KD and control groups.
(B) Longitudinal flow cytometry analyses reveal an increase of Treg and CM CD4+ T cell subsets after IVIG therapy. Conversely, PD1+ Tregs cells exhibit a tendency to decrease. Violin plots depict group distributions, and each line connecting KD timepoints represents the protein level trajectory for an individual patient.
(C) Spearman correlation analysis demonstrates the relationship between baseline PD1+ Treg levels and APBB1IP, TGFA, and OSM proteins, with the regression line displayed in black.
(D) Differentially expressed genes ranked by p-value and fold change in sorted EM CD4+ T cells and E) CM CD4+ T cells between acute KD children and the FC.
(F) Longitudinal alterations in gene expression post IVIG therapy within EM CD4+ T cell and Treg subsets.

potential benefit of replicating this analysis on a larger dataset. Such an endeavor may prove valuable in distinguishing KD from other mimicking conditions.

4. Discussion

Considerable efforts have been made in the research of KD; but still many pivotal questions remain unresolved. The limited knowledge in these areas hinders the development of diagnostic or prognostic test, as well as advance in the treatment of IVIG resistant patients. Cellular immune dysfunction underlying such conditions has been only partially understood, often with conflicting results [8,35].

Our analysis shows that the cytokine storm is modulated during the acute phase by the administration of IVIG. We explored the longitudinal proteomic dynamics of children with KD, identifying DEPs which inform a novel list of candidate proteins for diagnosis and prognosis. The cytokine storm observed in KD was characterized by elevated levels of CXCL10, CXCL9, IL-6, IL-17 A, IL-17C, IL-10.

In addition, our analysis also highlighted TNF superfamily members 12 (TNFSF12) and IL-6 to be upregulated DEPs in KD compared to FC and HC. In line with this, previous findings also showed that those pathways, out of a 13 gene expression signature, were able to distinguish KD from FC [13].

We further confirmed the pathogenic role of IL-17 A [30,31]. Specifically, the elevated levels of Th17 mediators such as IL-17 A, along with increased Th1 downstream mediators as TNF-α and CXCL10 in KD, indicate potential targets for intervention. Thus, considering the use of Secukinumab or Ixekizumab to target IL-17 A or employing anti-TNFα treatments could be valuable strategies, especially for KD children with IVIG resistance or in groups considered at "higher risk".

Nonetheless, our findings brought to light the significance of CCL7, which serves as a potent chemotactic factor for monocytes and neutrophils, playing a critical role in the pathogenesis of cardiovascular and inflammatory diseases [36,37]. Moreover, this chemokine is overexpressed in cardiac fibroblasts of mouse model of KD [38] and it is emerging as a key player in the pathogenesis of aortic aneurysms [39,40].

To further explore prognosis correlations, clinical characteristics including CAI were analyzed in association with protein level at baseline. The impact of age was confirmed by the correlation plot: indeed, most proteins involved in the cytokine storm and possibly underlying the disease course were inversely related to age, further confirming what literature knows very well, that the youngest are at higher risk for disease complications [41]. This observation further provides molecular evidence that this specific group may deserve a distinct clinical management with a combined "first line" therapeutic approach that combines high dose of IVIG with other immunosuppressive treatments (e.g. CS, anti-TNF-a) [14,41].

The analysis further revealed a positive association between dilated coronary artery *Z*-score and APBB1IP. The same trend was found also for RCA, LAD and LM value expressed in mm. Such protein resulted significantly higher in CAI+ patients, suggesting a potentially pivotal role for this protein in informing and possibly predicting CAI in KD. APBB1IP, also known as RIAM, is required for neutrophil migration, adhesion, extravasation, and polarity in response to chemokines, and is crucial for the cooperative actions of neutrophils and platelets in producing neutrophil extracellular traps, as well as for NK cell cytotoxicity [42]. Moreover, through its various domains, APBB1IP is a critical node

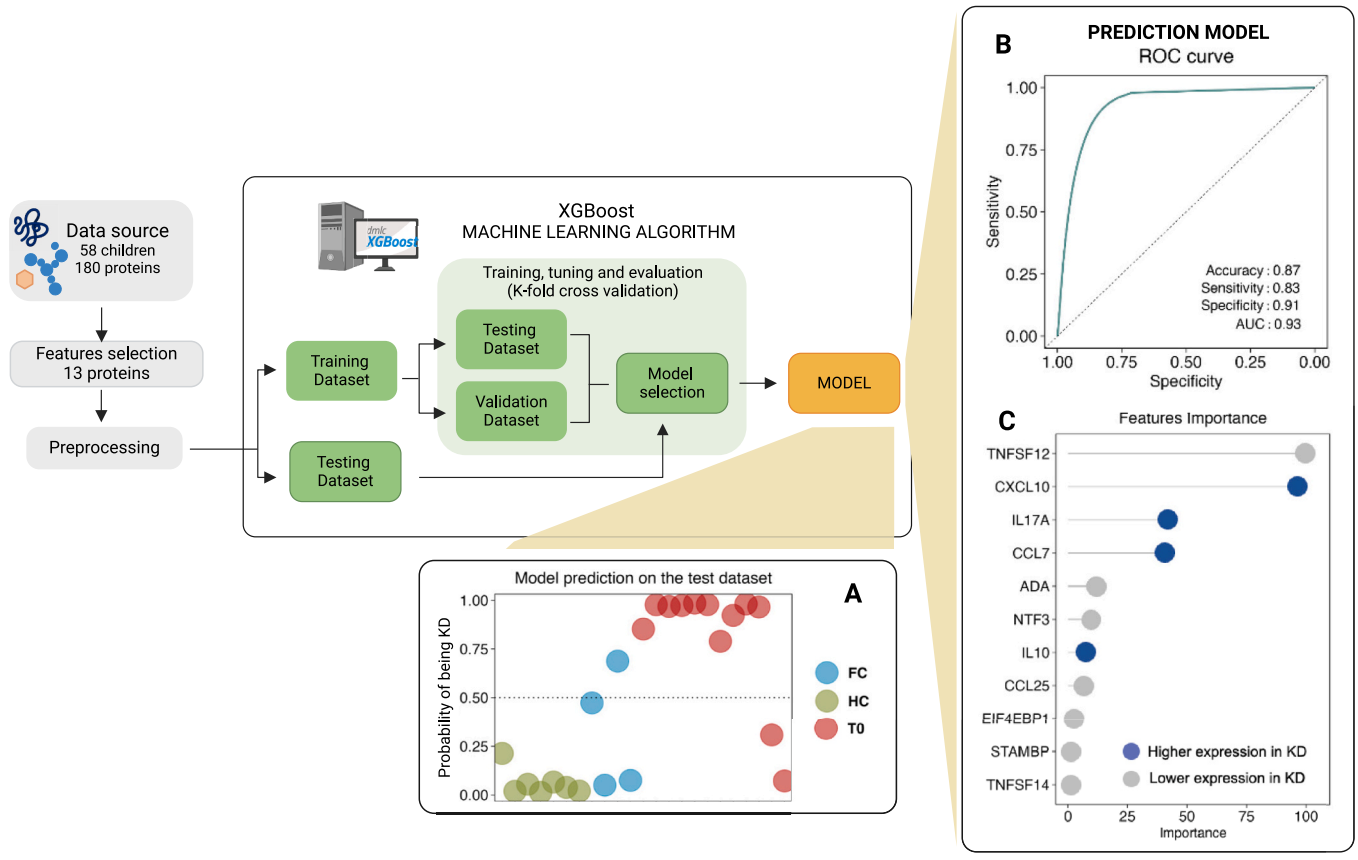

Fig. 4. Machine Learning Model.
The cartoon illustrates the stepwise progression in constructing a predictive model able to distinguish KD patients from the control groups. Four machine learning algorithms were evaluated, encompassing Logistic Regression, Random Forest, eXtreme Gradient Boosting (XGBoost), and knearest neighbor ($k-$NN). The assessment of the models' performance entailed computing accuracy, sensitivity, and specificity on the testing dataset. A) The model showing the best performance was built using the eXtreme Gradient Boosting (XGBoost) algorithm. B) The performance metrics are displayed in the upper right quadrant of the ROC curve. C) The lower right quadrant provides a visual representation of the features importance ranking employed within the model. Of note, proteins were colored in blue if upregulated in KD children respect to the control groups and in gray if downregulated. (For interpretation of the references to colour in this figure legend, the reader is referred to the web version of this article.)

of signal integration for activation of T cells [43]. Interestingly, APBB1IP was linked to coronary artery disease in both mice and humans [44].

APBB1IP may enhance platelet activation, promoting their interaction and aggregation with monocytes and neutrophils. These leukocyte–platelet aggregates could exacerbate KD pathogenesis through their pro-inflammatory and thrombotic activities, potentially contributing to the development of coronary artery aneurysms [45]. Further studies should dissect its contribution in the immune cell's infiltration at coronary artery level in KD.

To investigate the contribution of the T cell compartment we analyzed T cell subsets at both quantitative and qualitative level. KD is characterized by decreased absolute T cell counts in peripheral blood as previously reported [35], downregulation of T cell receptor expression [11], reduced levels of Tregs and a notable increase in Th17 cells during the acute phase [7,22,46].

Our analysis showed a global perturbation within maturational subsets of the T cell compartment with lower naïve, EM, CM and pTfh CD4+ T cell subsets in the acute phase of the KD. A longitudinal evaluation of the T cell distribution mirrored findings from Franco et al., who identified a rapid expansion of circulating EM, CM and Treg cells after IVIG and over the convalescent phase [10].

The Treg compartment seems to play an important role especially after treatment intervention [7,22,46]. In this context we explored PD1 expression which can enhance FOXP3 expression, Treg function and de-novo generation of Treg [47].

An inverse association was found between APBB1IP, OSM and TGFA and PD1+ Treg cells over the acute phase of KD. This association reflects on a possible protection effect sustained by PD1 + Treg over the acute phase and it may represent a possible indicator of disease progression once confirmed by larger studies. In this context, it is unknown whether Tregs can be destabilized through a NOTCH1-dependent mechanism also in KD, as recently observed in MIS-C [48].

From a longitudinal perspective, we highlighted the ability of IVIG in inducing an increase in Treg frequency, and to enhance the gene expression of NFATc1 of these cells. Interestingly, NFATc1 signaling was previously shown to be able to promote Tregs stability and their suppressive function [28] as well as being a major molecular target for other immunosuppressive drugs such as cyclosporin A and tacrolimus [49,50]. In addition, genes involving the NFATs pathway have been identified as KD susceptibility genes [51]. Overall, these results further suggest that IVIG intervention provide anti-inflammatory effects through multiple mechanisms highlighted by proteomic, T cell compartment and gene expression dynamics. Further analysis able to integrate such multi-omics signatures will be needed to provide definitive diagnostic and prognostic biomarkers.

In this scenario, albeit limited by the small sample size, by employing a ML approach, we identified key proteins, which allow to distinguish KD from the control groups, achieving high accuracy in classification. Interestingly, in our study KD children had lower expression of TNFSF12 which is a stronger angiogenic regulator involved in the endothelial cell

survival and proliferation and CXCL10 which play roles in regulating T cells and inflammation [51].

Some limitations of this study should be mentioned. Firstly, the study cohort's sample size might be limited, which could impact the generalizability of the findings to a broader population. One of the major limitations of our findings is the enrollment of only Caucasian patients with no children of African and Asian ancestry. Moreover, our samples from KD children with CAI were limited. Our proteomic results may be biased by the selection of 180 proteins. Thus, the use of other high throughput proteomic assays could provide additional information. Furthermore, the key proteins identified lack validation in an independent cohort.

Nonetheless, this study directly delineated expression alterations in numerous inflammatory proteins and T cell subsets between KD and control groups, yielding valuable insights for future multi-omics research. Overall, the data presented, albeit to be confirmed in a large validation cohort, suggest the design of future studies, aiming to achieve a more mechanistic understanding of the immunopathology of KD and the identification of novel intervention targets.

Funding

This work was supported by the Italian Ministry of Health with "Current Research funds" to NC. This work was supported by the 5 × 1000 from the Italian Ministry of Health to DA.

Data and materials availability

Patient samples can be made available within the limits of the approved Ethical permits. Data should be directed to the lead contact author upon reasonable request.

Scripts to reproduce the analyses presented in each figure of the paper are available upon request.

CRediT authorship contribution statement

Nicola Cotugno: Writing – review & editing, Writing – original draft, Funding acquisition, Conceptualization. **Giulio Olivieri:** Writing – review & editing, Writing – original draft, Visualization, Data curation, Conceptualization. **Giuseppe Rubens Pascucci:** Software, Investigation, Formal analysis. **Donato Amodio:** Writing – review & editing, Methodology, Investigation. **Elena Morrocchi:** Writing – review & editing, Methodology. **Chiara Pighi:** Writing – review & editing, Investigation. **Emma Concetta Manno:** Writing – review & editing, Resources, Investigation. **Gioacchino Andrea Rotulo:** Writing – review & editing, Investigation. **Carolina D'Anna:** Writing – review & editing, Investigation. **Marcello Chinali:** Writing – review & editing, Investigation. **Isabella Tarissi de Jacobis:** Writing – review & editing, Investigation. **Danilo Buonsenso:** Writing – review & editing, Investigation. **Alberto Villani:** Writing – review & editing, Investigation. **Paolo Rossi:** Writing – review & editing, Funding acquisition. **Alessandra Marchesi:** Writing – review & editing, Investigation. **Paolo Palma:** Writing – review & editing, Visualization, Supervision, Project administration, Funding acquisition.

Declaration of competing interest

The authors declare that they have no known competing financial interests or personal relationships that could have appeared to influence the work reported in this paper.

Data availability

Data will be made available on request.

Acknowledgments

We would like to acknowledge all patients and guardians who decided to participate in the study. We acknowledge Jennifer Faudella, Ilaria Pepponi, and Melania Fantini for administrative assistance and Tamara Di Marco and Nadia Iavarone as professional study nurses. We further acknowledge Salvatore Rocca.

Appendix A. Supplementary data

Supplementary data to this article can be found online at https://doi.org/10.1016/j.clim.2024.110349.

References

[1] J.W. Newburger, M. Takahashi, J.C. Burns, Kawasaki disease, J. Am. Coll. Cardiol. 67 (2016) 1738–1749, https://doi.org/10.1016/j.jacc.2015.12.073.

[2] A.H. Tremoulet, B.M. Best, S. Song, S. Wang, E. Corinaldesi, J.R. Eichenfield, D. D. Martin, J.W. Newburger, J.C. Burns, Resistance to intravenous immunoglobulin in children with Kawasaki disease, J. Pediatr. 153 (2008) 117–121, https://doi.org/10.1016/j.jpeds.2007.12.021.

[3] B.W. McCrindle, A.H. Rowley, J.W. Newburger, J.C. Burns, A.F. Bolger, M. Gewitz, A.L. Baker, M.A. Jackson, M. Takahashi, P.B. Shah, T. Kobayashi, M.-H. Wu, T. T. Saji, E. Pahl, American Heart Association rheumatic fever, endocarditis, and Kawasaki disease Committee of the Council on cardiovascular disease in the young; council on cardiovascular and stroke nursing; council on cardiovascular surgery and anesthesia; and council on epidemiology and prevention, diagnosis, treatment, and long-term Management of Kawasaki Disease: a scientific statement for health professionals from the American Heart Association, Circulation 135 (2017) e927–e999, https://doi.org/10.1161/CIR.0000000000000484.

[4] B.W. McCrindle, A.H. Rowley, Improving coronary artery outcomes for children with Kawasaki disease, Lancet Lond. Engl. 393 (2019) 1077–1078, https://doi.org/10.1016/S0140-6736(18)33133-7.

[5] K.G. Friedman, K. Gauvreau, A. Hamaoka-Okamoto, A. Tang, E. Berry, A. H. Tremoulet, V.S. Mahavadi, A. Baker, S.D. deFerranti, D.R. Fulton, J.C. Burns, J. W. Newburger, Coronary artery aneurysms in Kawasaki disease: risk factors for progressive disease and adverse cardiac events in the US population, J. Am. Heart Assoc. 5 (2016) e003289, https://doi.org/10.1161/JAHA.116.003289.

[6] J.C. Burns, A. Franco, The immunomodulatory effects of intravenous immunoglobulin therapy in Kawasaki disease, expert rev, Clin. Immunol. 11 (2015) 819–825, https://doi.org/10.1586/1744666X.2015.1044980.

[7] S. Jia, C. Li, G. Wang, J. Yang, Y. Zu, The T helper type 17/regulatory T cell imbalance in patients with acute Kawasaki disease, Clin. Exp. Immunol. 162 (2010) 131–137, https://doi.org/10.1111/j.1365-2249.2010.04236.x.

[8] T. Matsubara, T. Ichiyama, S. Furukawa, Immunological profile of peripheral blood lymphocytes and monocytes/macrophages in Kawasaki disease, Clin. Exp. Immunol. 141 (2005) 381–387, https://doi.org/10.1111/j.1365-2249.2005.02821.x.

[9] M. Xu, Y. Jiang, J. Wang, D. Liu, S. Wang, H. Yi, S. Yang, Distribution of distinct subsets of circulating T follicular helper cells in Kawasaki disease, BMC Pediatr. 19 (2019) 43, https://doi.org/10.1186/s12887-019-1412-z.

[10] A. Franco, C. Shimizu, A.H. Tremoulet, J.C. Burns, Memory T-cells and characterization of peripheral T-cell clones in acute Kawasaki disease, Autoimmunity 43 (2010) 317–324, https://doi.org/10.3109/08916930903405891.

[11] T. Kusuda, Y. Nakashima, K. Murata, S. Kanno, H. Nishio, M. Saito, T. Tanaka, K. Yamamura, Y. Sakai, H. Takada, T. Miyamoto, Y. Mizuno, K. Ouchi, K. Waki, T. Hara, Kawasaki disease-specific molecules in the sera are linked to microbe-associated molecular patterns in the biofilms, PLoS One 9 (2014) e113054, https://doi.org/10.1371/journal.pone.0113054.

[12] Y. Hirabayashi, Y. Takahashi, Y. Xu, K. Akane, I.B. Villalobos, Y. Okuno, S. Hasegawa, H. Muramatsu, A. Hama, T. Kato, S. Kojima, Lack of $CD4^{+}CD25^{+}FOXP3^{+}$ regulatory T cells is associated with resistance to intravenous immunoglobulin therapy in patients with Kawasaki disease, Eur. J. Pediatr. 172 (2013) 833–837, https://doi.org/10.1007/s00431-013-1937-3.

[13] V.J. Wright, J.A. Herberg, M. Kaforou, C. Shimizu, H. Eleftherohorinou, H. Shailes, A.M. Barendregt, S. Menikou, S. Gormley, M. Berk, L.T. Hoang, A.H. Tremoulet, J. T. Kanegaye, L.J.M. Coin, M.P. Glodé, M. Hibberd, T.W. Kuijpers, C.J. Hoggart, J. C. Burns, M. Levin, Immunopathology of respiratory, inflammatory and infectious disease study (IRIS) consortium and the pediatric emergency medicine Kawasaki disease research group (PEMKDRG), diagnosis of kawasaki disease using a minimal whole-blood gene expression signature, JAMA Pediatr. 172 (2018) e182293, https://doi.org/10.1001/jamapediatrics.2018.2293.

[14] A. Marchesi, D. Rigante, R. Cimaz, A. Ravelli, I. Tarissi de Jacobis, A. Rimini, F. Cardinale, M. Cattalini, A. De Zorzi, R.M. Dellepiane, P. Salice, A. Secinaro, A. Taddio, P. Palma, M. El Hachem, E. Cortis, M.C. Maggio, G. Corsello, A. Villani, Revised recommendations of the Italian Society of Pediatrics about the general management of Kawasaki disease, Ital. J. Pediatr. 47 (2021) 16, https://doi.org/10.1186/s13052-021-00962-4.

[15] E. Assarsson, M. Lundberg, G. Holmquist, J. Björkesten, S.B. Thorsen, D. Ekman, A. Eriksson, E. Rennel Dickens, S. Ohlsson, G. Edfeldt, A.-C. Andersson, P. Lindstedt, J. Stenvang, M. Gullberg, S. Fredriksson, Homogenous 96-plex PEA

immunoassay exhibiting high sensitivity, specificity, and excellent scalability, PLoS One 9 (2014) e95192, https://doi.org/10.1371/journal.pone.0095192.
[16] N. Cotugno, S. Zicari, E. Morrocchi, L.R. de Armas, S. Pallikkuth, S. Rinaldi, A. Ruggiero, E.C. Manno, P. Zangari, M. Chiriaco, S. Bernardi, S.F. Andrews, A. Cagigi, P. Rossi, A.B. McDermott, S. Pahwa, P. Palma, Higher PIK3C2B gene expression of H1N1+ specific B-cells is associated with lower H1N1 immunogenicity after trivalent influenza vaccination in HIV infected children, Clin. Immunol. Orlando Fla 215 (2020) 108440, https://doi.org/10.1016/j.clim.2020.108440.
[17] B.M. Bolstad, R.A. Irizarry, M. Astrand, T.P. Speed, A comparison of normalization methods for high density oligonucleotide array data based on variance and bias, Bioinforma. Oxf. Engl. 19 (2003) 185–193, https://doi.org/10.1093/bioinformatics/19.2.185.
[18] D. Türei, A. Valdeolivas, L. Gul, N. Palacio-Escat, M. Klein, O. Ivanova, M. Ölbei, A. Gábor, F. Theis, D. Módos, T. Korcsmáros, J. Saez-Rodriguez, Integrated intra- and intercellular signaling knowledge for multicellular omics analysis, Mol. Syst. Biol. 17 (2021) e9923, https://doi.org/10.15252/msb.20209923.
[19] R. Argelaguet, D. Arnol, D. Bredikhin, Y. Deloro, B. Velten, J.C. Marioni, O. Stegle, MOFA+: a statistical framework for comprehensive integration of multi-modal single-cell data, Genome Biol. 21 (2020) 111, https://doi.org/10.1186/s13059-020-02015-1.
[20] C.M. Bishop, Model-based machine learning, Philos. Transact. A math. Phys, Eng. Sci. 371 (2013) 20120222, https://doi.org/10.1098/rsta.2012.0222.
[21] C.-M. Tsai, C.-H.R. Lin, H.-C. Kuo, F.-J. Cheng, H.-R. Yu, T.-C. Hung, C.-S. Hung, C.-M. Huang, Y.-C. Chu, Y.-H. Huang, Use of machine learning to differentiate children with Kawasaki disease from other febrile children in a pediatric emergency department, JAMA Netw. Open 6 (2023) e237489, https://doi.org/10.1001/jamanetworkopen.2023.7489.
[22] M.M.-H. Guo, W.-N. Tseng, C.-H. Ko, H.-M. Pan, K.-S. Hsieh, H.-C. Kuo, Th17- and Treg-related cytokine and mRNA expression are associated with acute and resolving Kawasaki disease, Allergy 70 (2015) 310–318, https://doi.org/10.1111/all.12558.
[23] D. Foell, F. Ichida, T. Vogl, X. Yu, R. Chen, T. Miyawaki, C. Sorg, J. Roth, S100A12 (EN-RAGE) in monitoring Kawasaki disease, Lancet Lond. Engl. 361 (2003) 1270–1272, https://doi.org/10.1016/S0140-6736(03)12986-8.
[24] F. Ye, D. Foell, K. Hirono, T. Vogl, C. Rui, X. Yu, S. Watanabe, K. Watanabe, K. Uese, I. Hashimoto, J. Roth, F. Ichida, T. Miyawaki, Neutrophil-derived S100A12 is profoundly upregulated in the early stage of acute Kawasaki disease, Am. J. Cardiol. 94 (2004) 840–844, https://doi.org/10.1016/j.amjcard.2004.05.076.
[25] J.J. Rodriguez-Smith, E.L. Verweyen, G.M. Clay, Y.M. Esteban, S.R. de Loizaga, E. J. Baker, T. Do, S. Dhakal, S.M. Lang, A.A. Grom, D. Grier, G.S. Schulert, Inflammatory biomarkers in COVID-19-associated multisystem inflammatory syndrome in children, Kawasaki disease, and macrophage activation syndrome: a cohort study, lancet, Rheumatol 3 (2021) e574–e584, https://doi.org/10.1016/S2665-9913(21)00139-9.
[26] Y. Collette, A. Gilles, P. Pontarotti, D. Olive, A co-evolution perspective of the TNFSF and TNFRSF families in the immune system, Trends Immunol. 24 (2003) 387–394, https://doi.org/10.1016/s1471-4906(03)00166-2.
[27] C.-Y. Chen, S.-H. Huang, K.-J. Chien, T.-J. Lai, W.-H. Chang, K.-S. Hsieh, K.-P. Weng, Reappraisal of VEGF in the pathogenesis of Kawasaki disease, Child. Basel Switz. 9 (2022) 1343, https://doi.org/10.3390/children9091343.
[28] Y. Wu, M. Borde, V. Heissmeyer, M. Feuerer, A.D. Lapan, J.C. Stroud, D.L. Bates, L. Guo, A. Han, S.F. Ziegler, D. Mathis, C. Benoist, L. Chen, A. Rao, FOXP3 controls regulatory T cell function through cooperation with NFAT, Cell 126 (2006) 375–387, https://doi.org/10.1016/j.cell.2006.05.042.
[29] S. Chuvpilo, A. Avots, F. Berberich-Siebelt, J. Glöckner, C. Fischer, A. Kerstan, C. Escher, I. Inashkina, F. Hlubek, E. Jankevics, T. Brabletz, E. Serfling, Multiple NF-ATc isoforms with individual transcriptional properties are synthesized in T lymphocytes, J. Immunol. Baltim. Md. 1950 (162) (1999) 7294–7301.
[30] K.E. Brodeur, M. Liu, D. Ibanez, M.J. de Groot, L. Chen, Y. Du, E. Seyal, R. Laza-Briviesca, A. Baker, J.C. Chang, M.H. Chang, M. Day-Lewis, F. Dedeoglu, A. Dionne, S.D. de Ferranti, K.G. Friedman, O. Halyabar, M.S. Lo, E. Meidan, R. P. Sundel, L.A. Henderson, P.A. Nigrovic, J.W. Newburger, M.B. Son, P.Y. Lee, Elevation of IL-17 cytokines distinguishes Kawasaki disease from other pediatric inflammatory disorders, Arthritis Rheumatol. Hoboken NJ (2023), https://doi.org/10.1002/art.42680.
[31] C.R. Consiglio, N. Cotugno, F. Sardh, C. Pou, D. Amodio, L. Rodriguez, Z. Tan, S. Zicari, A. Ruggiero, G.R. Pascucci, V. Santilli, T. Campbell, Y. Bryceson, D. Eriksson, J. Wang, A. Marchesi, T. Lakshmikanth, A. Campana, A. Villani, P. Rossi, CACTUS Study Team, N. Landegren, P. Palma, P. Brodin, The immunology of multisystem inflammatory syndrome in children with COVID-19, Cell 183 (2020), https://doi.org/10.1016/j.cell.2020.09.016, 968–981.e7.
[32] Y. Li, Q. Zheng, L. Zou, J. Wu, L. Guo, L. Teng, R. Zheng, L.K.L. Jung, M. Lu, Kawasaki disease shock syndrome: clinical characteristics and possible use of IL-6, IL-10 and IFN-γ as biomarkers for early recognition, Pediatr. Rheumatol. Online J. 17 (2019) 1, https://doi.org/10.1186/s12969-018-0303-4.
[33] J. Hirao, S. Hibi, T. Andoh, T. Ichimura, High levels of circulating interleukin-4 and interleukin-10 in Kawasaki disease, Int. Arch. Allergy Immunol. 112 (1997) 152–156, https://doi.org/10.1159/000237447.
[34] S.R. Wiley, J.A. Winkles, TWEAK, a member of the TNF superfamily, is a multifunctional cytokine that binds the TweakR/Fn14 receptor, Cytokine Growth Factor Rev. 14 (2003) 241–249, https://doi.org/10.1016/s1359-6101(03)00019-4.
[35] Z. Xie, Y. Huang, X. Li, Y. Lun, X. Li, Y. He, S. Wu, S. Wang, J. Sun, J. Zhang, Atlas of circulating immune cells in Kawasaki disease, Int. Immunopharmacol. 102 (2022) 108396, https://doi.org/10.1016/j.intimp.2021.108396.
[36] T.-T. Chang, C. Chen, J.-W. Chen, CCL7 as a novel inflammatory mediator in cardiovascular disease, diabetes mellitus, and kidney disease, Cardiovasc. Diabetol. 21 (2022) 185, https://doi.org/10.1186/s12933-022-01626-1.
[37] P.M. Brunner, E. Glitzner, B. Reininger, I. Klein, G. Stary, M. Mildner, P. Uhrin, M. Sibilia, G. Stingl, CCL7 contributes to the TNF-alpha-dependent inflammation of lesional psoriatic skin, Exp. Dermatol. 24 (2015) 522–528, https://doi.org/10.1111/exd.12709.
[38] A.T. Stock, J.A. Hansen, M.A. Sleeman, B.S. McKenzie, I.P. Wicks, GM-CSF primes cardiac inflammation in a mouse model of Kawasaki disease, J. Exp. Med. 213 (2016) 1983–1998, https://doi.org/10.1084/jem.20151853.
[39] C. Xie, F. Ye, N. Zhang, Y. Huang, Y. Pan, X. Xie, CCL7 contributes to angiotensin II-induced abdominal aortic aneurysm by promoting macrophage infiltration and pro-inflammatory phenotype, J. Cell. Mol. Med. 25 (2021) 7280–7293, https://doi.org/10.1111/jcmm.16757.
[40] C.-L. Tsou, W. Peters, Y. Si, S. Slaymaker, A.M. Aslanian, S.P. Weisberg, M. Mack, I. F. Charo, Critical roles for CCR2 and MCP-3 in monocyte mobilization from bone marrow and recruitment to inflammatory sites, J. Clin. Invest. 117 (2007) 902–909, https://doi.org/10.1172/JCI29919.
[41] H. Wang, C. Shimizu, E. Bainto, S. Hamilton, H.R. Jackson, D. Estrada-Rivadeneyra, M. Kaforou, M. Levin, J.M. Pancheri, K.B. Dummer, A.H. Tremoulet, J.C. Burns, Subgroups of children with Kawasaki disease: a data-driven cluster analysis, lancet child Adolesc, Health 7 (2023) 697–707, https://doi.org/10.1016/S2352-4642(23)00166-9.
[42] N. Patsoukis, K. Bardhan, J.D. Weaver, D. Sari, A. Torres-Gomez, L. Li, L. Strauss, E. M. Lafuente, V.A. Boussiotis, The adaptor molecule RIAM integrates signaling events critical for integrin-mediated control of immune function and cancer progression, Sci. Signal. 10 (2017) eaam8298, https://doi.org/10.1126/scisignal.aam8298.
[43] Q. Ge, G. Li, J. Chen, J. Song, G. Cai, Y. He, X. Zhang, H. Liang, Z. Ding, B. Zhang, Immunological role and prognostic value of APBB1IP in Pan-Cancer analysis, J. Cancer 12 (2021) 595–610, https://doi.org/10.7150/jca.50785.
[44] Z. Kurt, J. Cheng, C.N. McQuillen, Z. Saleem, N. Hsu, N. Jiang, R. Barrere-Cain, C. Pan, O. Franzen, S. Koplev, S. Wang, J. Bjorkegren, A.J. Lusis, M. Blencowe, X. Yang, Shared and distinct pathways and networks genetically linked to coronary artery disease between human and mouse, BioRxiv Prepr. Serv. Biol. (2023), https://doi.org/10.1101/2023.06.08.544148, 2023.06.08.544148.
[45] M. Noval Rivas, B. Kocatürk, B.S. Franklin, M. Arditi, Platelets in Kawasaki disease: mediators of vascular inflammation, Nat. Rev. Rheumatol. (2024), https://doi.org/10.1038/s41584-024-01119-3.
[46] B. Olivito, A. Taddio, G. Simonini, C. Massai, S. Ciullini, E. Gambineri, M. de Martino, C. Azzari, R. Cimaz, Defective FOXP3 expression in patients with acute Kawasaki disease and restoration by intravenous immunoglobulin therapy, Clin. Exp. Rheumatol. 28 (2010) 93–97.
[47] L.M. Francisco, P.T. Sage, A.H. Sharpe, The PD-1 pathway in tolerance and autoimmunity, Immunol. Rev. 236 (2010) 219–242, https://doi.org/10.1111/j.1600-065X.2010.00923.x.
[48] M. Benamar, Q. Chen, J. Chou, A.M. Julé, R. Boudra, P. Contini, E. Crestani, P. S. Lai, M. Wang, J. Fong, S. Rockwitz, P. Lee, T.M.F. Chan, E.Z. Altun, E. Kepenekli, E. Karakoc-Aydiner, A. Ozen, P. Boran, F. Aygun, P. Onal, A.A.K. Sakalli, H. Cokugras, M.Y. Gelmez, F.B. Oktelik, E.A. Cetin, Y. Zhong, M.L. Taylor, K. Irby, N.B. Halasa, E.H. Mack, Overcoming COVID-19 Investigators, S. Signa, I. Prigione, M. Gattorno, N. Cotugno, D. Amodio, R.S. Geha, M.B. Son, J. Newburger, P. B. Agrawal, S. Volpi, P. Palma, A. Kiykim, A.G. Randolph, G. Deniz, S. Baris, R. De Palma, K. Schmitz-Abe, L.-M. Charbonnier, L.A. Henderson, T.A. Chatila, The Notch1/CD22 signaling axis disrupts Treg function in SARS-CoV-2-associated multisystem inflammatory syndrome in children, J. Clin. Invest. 133 (2023) e163235, https://doi.org/10.1172/JCI163235.
[49] K.T. Shaw, A.M. Ho, A. Raghavan, J. Kim, J. Jain, J. Park, S. Sharma, A. Rao, P. G. Hogan, Immunosuppressive drugs prevent a rapid dephosphorylation of transcription factor NFAT1 in stimulated immune cells, Proc. Natl. Acad. Sci. USA 92 (1995) 11205–11209, https://doi.org/10.1073/pnas.92.24.11205.
[50] O. Maguire, K.M. Tornatore, K.L. O'Loughlin, R.C. Venuto, H. Minderman, Nuclear translocation of nuclear factor of activated T cells (NFAT) as a quantitative pharmacodynamic parameter for tacrolimus, Cytom. Part J. Int. Soc. Anal. Cytol. 83 (2013) 1096–1104, https://doi.org/10.1002/cyto.a.22401.
[51] T.-M. Ko, H.-C. Kuo, J.-S. Chang, S.-P. Chen, Y.-M. Liu, H.-W. Chen, F.-J. Tsai, Y.-C. Lee, C.-H. Chen, J.-Y. Wu, Y.-T. Chen, CXCL10/IP-10 is a biomarker and mediator for Kawasaki disease, Circ. Res. 116 (2015) 876–883, https://doi.org/10.1161/CIRCRESAHA.116.305834.